

A novel approach with “skeletonised MTR” measures tract-specific microstructural changes in early primary-progressive MS

B. Bodini^{1*}, M. Cercignani^{2,3*}, A. Toosy¹, N. De Stefano⁴, D.H. Miller⁴, A.J. Thompson¹ and O. Ciccarelli¹

¹Department of Brain Repair and Rehabilitation and ⁴Neuroinflammation, University College London Institute of Neurology, Queen Square, London, UK; ²Neuroimaging Laboratory, IRCCS Santa Lucia Foundation, Rome, Italy; ³Clinical Imaging Science Centre, Brighton and Sussex Medical School, Brighton, UK; ⁴Department of Neurological and Behavioural Sciences, University of Siena, Siena, Italy

*Both Authors contributed equally to this work

This study was performed at the University College London Institute of Neurology, Queen Square, London, United Kingdom, WC1N 3BG.

Corresponding author: Dr Benedetta Bodini, Department of Brain Repair and Rehabilitation, UCL Institute of Neurology, Queen Square, London WC1N 3BG, UK, Tel : +44 (0) 20344884307; Fax : +44 (0) 207 813 6505; E-mail: b.bodini@ucl.ac.uk

Abstract

We combined tract-based spatial statistics (TBSS) and magnetization transfer (MT) imaging to assess white matter (WM) tract-specific short-term changes in early primary-progressive multiple sclerosis (PPMS), and their relationships with clinical progression.

Twenty-one PPMS patients underwent MT and diffusion tensor imaging (DTI) at baseline (within 5 years from onset) and after 12 months. Patients' disability was assessed. DTI data were processed to compute fractional anisotropy (FA), and to generate a common WM "skeleton", which represents the tracts that are "common" to all subjects, using TBSS. The MT ratio (MTR) was computed from MT data and co-registered with the DTI. The skeletonisation procedure derived for FA was applied to each subject's MTR image to obtain a "skeletonised" MTR map for every subject. Permutation tests were used to assess (i) changes in FA, principal diffusivities and MTR over the follow-up, and (ii) associations between changes in imaging parameters and changes in disability.

Patients showed significant decreases in MTR over one year in the corpus callosum (CC), bilateral cortico-spinal tract (CST), thalamic radiations, and superior and inferior longitudinal fasciculi. These changes were located both within lesions and the normal-appearing WM. No significant longitudinal change in skeletonised FA was found, but radial diffusivity (RD) significantly increased in several regions, including the CST bilaterally and the right inferior longitudinal

fasciculus. MTR decreases, RD increases and AD decreases in the CC and CST correlated with deterioration in upper limb function.

We detected tract-specific multi-modal imaging changes that reflect the accrual of microstructural damage and possibly contribute to clinical impairment in PPMS. We propose a novel methodology that can be extended to other diseases to map cross-subject and tract-specific changes in MTR.

Introduction:

Magnetization transfer (MT) magnetic resonance imaging (MRI) has proved valuable in identifying and quantifying in-vivo pathologically relevant tissue changes in patients with multiple sclerosis (MS), including demyelination and remyelination, that occur within and outside visible lesions on T2-weighted scans (Ropele and Fazekas, 2009). Decreased MT ratio (MTR) values, which post-mortem studies have shown to be sensitive to a reduced myelin content, in addition to axonal loss (Schmierer et al., 2004), have been demonstrated in patients with relapsing-remitting and progressive forms of MS when compared with controls, since the early stages of the disease (Filippi and Agosta, 2010).

Previous MTR studies in patients with MS have employed histograms in *a priori* selected areas, such as segmentation-based masks or hand-drawn regions (Filippi and Agosta, 2010). More recently, tract-specific MTR changes have been measured using tractography-based strategies that determine the white matter (WM) tract of interest, both in healthy controls and in patients with psychiatric and neurological disorders (Dalby et al., 2010; de Zeeuw et al., 2011; Lin et al., 2008; Reich et al., 2006; Reich et al., 2007). However, tractography-based region-of-interest (ROI) approaches do not allow the whole brain to be investigated, and require the *a priori* selection of the tract(s) of interest. Tract-based spatial statistics (TBSS) is a fully automated, voxel-wise method that is able to carry out voxel-wise cross-subject statistics on diffusion derived metrics without requiring

an a priori hypothesis (Smith et al., 2006). By addressing the challenges of inter-subject data alignment, TBSS has been widely employed to localise WM changes related to normal brain development (Giorgio et al., 2008) and aging (Giorgio et al., 2010), as well as neurological diseases, including Alzheimer's disease (Damoiseaux et al., 2009; Serra et al., 2010; Stricker et al., 2009), epilepsy (Focke et al., 2008; Nguyen et al., 2011), and MS (Bodini et al., 2009; Kern et al., 2011; Raz et al., 2010). In particular, TBSS uses each subject's FA to produce an alignment-invariant tract structure, representing the core of whole-brain WM tracts, known as the "skeleton". This step is followed by the projection of FA values from the main WM tracts of every subject onto the skeleton, achieved by searching perpendicular to the local skeleton structure for the maximum FA value. This value is assumed to represent the nearest relevant tract centre. This step ensures the alignment of WM tracts rather than that of macroscopic features (e.g. the boundary between tissues or the sulci shape, as in standard voxel-based approaches).

Here we used TBSS to create an FA-based "skeleton", and then we applied the same "projection" procedure to co-registered MTR data to create a "skeletonised" MTR map for every subject. We employed this novel approach to explore the microstructural abnormalities reflected by one year changes in diffusion-derived parameters and MTR values along the core of WM tracts, within and outside T2 lesions, in patients with the early primary-progressive MS. We also aimed to

assess whether these WM changes were clinically relevant, by performing correlations with changes in clinical scores over the same follow-up.

Methods

Patients

Twenty-one patients diagnosed with PPMS according to Thompson's criteria (Thompson et al., 2000) (11 women, 10 men, mean age 46.6 yrs, SD 9.6), within 5 years of symptom onset, underwent a neurological assessment and a whole brain imaging protocol, including diffusion weighted imaging and MT imaging, at both study entry and after 12 months. These patients were part of a larger cohort of 50 subjects. A subset had diffusion and MT data at both, baseline and year 1, and was included in the current study. One patient was being treated with oral corticosteroids every four months. Clinical assessment included measuring the Expanded Disability Status Scale (EDSS) (Kurtzke, 1983), and the Multiple Sclerosis Functional Composite (MSFC) subtests (Cutter et al., 1999): Paced Auditory Serial Addition Test (PASAT), Nine-Hole peg Test (NHPT), and Timed Walk Test (TWT). The study was approved by the Joint Medical Ethics Committee of the National Hospital for Neurology and Neurosurgery and the UCL Institute of Neurology, London. Written and informed consent was obtained from all participants.

Image acquisition

Patients were imaged using a 1.5T GE Signa scanner (General Electrics, Milwaukee, IL). MRI acquisition and protocol were as follows:

(a) Three-dimensional inversion-recovery fast spoiled gradient recall (3D FSPGR) T1-weighted sequence of the brain (FOV 300x225 mm, matrix size 256x160 (reconstructed to 256x256 for a final in plane resolution of 1.17 mm), repetition time 13.3 ms, echo time 4.2 ms, inversion time 450 ms, 124 axial slices, 1.5 mm thickness).

(b) Whole-brain, cardiac-gated, Spin Echo Diffusion-Weighted (DW) Echo Planar Imaging sequence [FOV 240x240mm², matrix size 96x96 (reconstructed to 128x128), image resolution 2.5x2.5x3mm (reconstructed to 1.9x1.9x3mm), TE 95ms, TR 7RRs, maximum b-factor 1000 smm⁻²; three series, each collecting 14 axial slices of 3mm thickness, which were interleaved off-line; diffusion gradients were applied along 25 optimised directions (Jones et al., 1999), and three images with no diffusion weighting were also acquired.

(c) Magnetisation transfer (MT) dual echo interleaved spin-echo sequence (Barker et al., 1996) (28 contiguous axial slices, repetition time [TR] 1720 ms, echo time [TEs] 30/80 ms, number of excitations [NEX] 0.75, acquired matrix 256x128, reconstructed matrix 256x256, field of view [FOV] 240x240 mm). We acquired 28 contiguous axial slices and a slice thickness of 5 mm. A Hamming-apodised three-lobe sinc MT pulse (duration 16 ms, peak amplitude 23.2 μ T,

bandwidth 250 Hz, 1 kHz off-water resonance) was used. The sequence collects inherently co-registered proton density (PD) (30 ms echo) and T2-weighted images (80 ms echo) before and after the saturation pulse.

Image post-processing

Lesions were delineated with a semi-automated contour thresholding technique (Plummer, 1992) by a single rater on the unsaturated PD images of the MT protocol. The T2-weighted images, which were inherently co-registered with the PD-weighted images (both acquired with the same dual-echo sequence), were always used as a visual reference to increase confidence in lesion identification. Lesion masks were obtained by setting the signal intensity equal to 1 for all voxels within a lesion and zero outside lesions. The same procedure was performed on the baseline and the follow-up scans.

After correction for eddy-current induced distortions, the diffusion tensor was calculated on a voxel-by-voxel basis, and FA maps were generated using DTIfit, that is part of the FMRIB Software Library 4.1 (FSL, FMRIB Image Analysis Group, Oxford, UK) (Smith et al., 2004).

FA maps were fed into Tract-Based Spatial Statistics (TBSS) (Smith et al., 2006), to generate a common FA tract skeleton onto which every subject's FA was then projected. This is achieved via the following steps. FA images are scalp-stripped

and then aligned to a common target (in this case the FSL FA template in MNI coordinates) using nonlinear registration (based on the tool FNIRT from the FSL library). The aligned images are averaged to produce a mean image, which is then thinned by non-maximum suppression perpendicular to the local tract structure, to create an alignment-invariant tract representation: the “skeleton”. Each subject’s FA is then projected onto the skeleton by searching perpendicular to the local skeleton structure for the maximum value in the subject’s FA image. As some animal work suggests that axial diffusivity (AD) (coincident with the largest eigenvalue of the diffusion tensor, i.e., diffusion coefficient along the direction of maximum diffusion) and radial diffusivity (RD) (the average diffusion coefficient in the orthogonal directions) are more specific than FA to microstructural changes involving axons and myelin, respectively (Song et al., 2005), we also performed a TBSS analysis of these indices (see Supplemental Material).

MTR maps were calculated from the inherently co-registered PD images of the MT sequence in native space, by subtracting the saturated from the unsaturated signal, using the formula $MTR = [(M_0 - M_s) / M_0] \times 100$ percent units (pu) on a pixel-by-pixel basis. These short-echo images were chosen because the resulting MTR map has higher signal-to-noise ratio than that from the 80-ms echo.

To obtain a “skeletonised” MTR image for each subject, MT data were first co-registered with DTI by matching the native non-MT weighted volume (inherently co-registered with the MTR maps) with the native b0 volume, after skull-stripping,

with an affine transformation using FLIRT (FMRIB's Linear Image Registration Tool, part of FSL), using normalised mutual information as the cost function. The transformation was then applied to the native MTR map. Finally, the transformed MTR map underwent the same projection as the FA data onto the common FA tract skeleton, to obtain a “skeletonised” MTR image in MNI space, for each subject at each time point.

Statistical analysis

Assessment of clinical progression over one year

To assess whether there was a significant deterioration in EDSS score over the follow-up period, the EDSS scores at baseline and at year one were compared using the Wilcoxon matched-pairs signed rank test. Changes in EDSS scores were then converted into steps by considering 1 step change equal to 1 point increase for values of EDSS of 5.5 or lower, and to 0.5 increase for values of EDSS higher than 5.5 (Wingerchuk et al., 1997). To measure if changes in MSFC subtests were significant over the follow-up, all the scores were first transformed into z-scores (z-NHPT, z-TWT and z-PASAT), using our baseline sample as reference. A paired t-test between the z-scores at the two time points was then performed for each MSFC subtest.

Changes in skeletonised FA and MTR over one year

To assess the presence of any regional change in FA and MTR over the follow-up period, the skeletonised FA and MTR maps and the skeletonised RD and AD maps at baseline (see supplemental material for the principal diffusivities) were compared with those at follow-up, using permutation tests (2000 iterations). Age, gender and disease duration at baseline were added as covariates of no interest. Correction for multiple comparisons was performed using threshold free cluster enhancement (TFCE) (Smith and Nichols, 2009). Differences were considered significant if $p < 0.05$.

Tract specific FA and MTR values were obtained and reported from every subject's skeletonised maps. The John Hopkins University white matter tractography atlas (Mori S et al., 2005) provided with FSL was used to identify the forceps major, the forceps minor, and 9 bilateral tracts: anterior thalamic radiation, cortico-spinal tract, cingulum bundle (split into cingulate and hippocampal parts), inferior fronto-occipital fasciculus, inferior longitudinal fasciculus, superior longitudinal fasciculus (split into fronto-parietal and temporal parts), and uncinate fasciculus.

Correlation between changes in FA and MTR and clinical changes over one year

In order to assess the association between the changes in FA (and principal diffusivities) and in MTR and the clinical variables, a map of the difference

between baseline and follow-up skeletonised images was computed for every patient.

(i) Correlation between FA and MTR changes and changes in EDSS

Patients were divided into three groups of similar size on the basis of their step-change in EDSS over one year: (1) patients who had no change in EDSS over the follow-up period; (2) patients whose EDSS step-change was equal to 0.5; (3) patients whose EDSS step-change was greater than 0.5. The voxel-wise FA (and principal diffusivities) and MTR differences between baseline and follow-up were regressed against the three groups of EDSS step-change to identify regions of significant correlation. Age, gender, and disease duration at baseline were included as additional covariates. Correction at $p < 0.05$ for multiple comparisons was performed using TFCE.

(ii) Correlation between FA and MTR changes and changes in MSFC subtests

To assess the correlation between the areas of FA (and principal diffusivities) and MTR change and the changes in MSFC subtests over one year, three linear multiple regression analyses were performed (one for each of the MSFC subtests), using the changes in z-NHPT, z-TWT and z-PASAT as regressors, and age, gender, and disease duration at baseline as covariates. TFCE was employed to correct at $p < 0.05$ for multiple comparisons.

Post-hoc analyses

(i) The role of lesions

To create a mask of “new and enlarged lesions” which developed during one-year follow-up, the lesion mask obtained from the T2-weighted images at baseline was subtracted lesion mask computed from the T2-weighted image at one year. This map includes both the new lesions, developed by patients during the follow-up period, and the portions of older lesions which have enlarged during follow-up. A lesion probability map was then created, in which a colour scale indicated the percentage of patients who had developed a new/enlarged lesion in a given voxel. To establish whether the areas of significant change in FA and MTR over one year were part of the “new/enlarged T2-weighted lesions” or were localised within the normal-appearing white matter (NAWM), the areas of significant decrease in FA and MTR, and the “new/enlarged T2-weighted lesion probability mask” were overlaid on the same anatomical image and then visually inspected.

Finally, to assess the contribution of the change in T2-weighted lesion load over the follow-up period to the significant changes found in the skeletonised FA/MTR, the lesion load increase over one year was first computed for each patient. Then, the correlation between the average skeletonised FA/MTR changes (i.e., the mean FA/MTR differences between baseline and one year in the areas that showed a significant change over one year) and the T2 lesion load difference was calculated, using Pearson’s correlation coefficient.

(ii) The role of total grey matter (GM) MTR

To assess the correlation between total GM MTR changes over one year and clinical changes during the same period, we computed the mean GM MTR value for each patient at each time point using the following procedure. First we used SPM8 (Ashburner and Friston, 2005) to segment the T1-weighted volumes into WM, GM and CSF in native space. The GM probability maps were thresholded (to retain only voxels with probability of more than 75% of belonging to the GM (Khaleeli et al., 2007a)), and binarised. These GM masks were applied to the whole brain MTR maps to obtain GM MTR maps. The mean GM MTR values were calculated for every patient at both baseline and follow-up. The difference between these two values (mean GM MTR at baseline – mean GM MTR at follow-up) was calculated. Finally, the correlations between GM MTR changes and clinical changes (i.e., changes in EDSS, NHPT, TWT, and PASAT) were assessed using Pearson's correlation coefficient.

(iii) Correlation between FA changes and MTR changes in regions that showed correlation between MTR changes and clinical function

To assess whether there was a correlation between FA and MTR changes in the regions that showed a significant association between MTR decrease and clinical changes, we extracted the mean skeletonised FA and MTR values from these areas at baseline and at follow-up, calculated the difference between these two values and tested for significant correlations between FA and MTR changes in

these regions using the Pearson's correlation coefficient (results with p values < 0.05 were considered significant). Similar analyses were performed on skeletonised AD and RD (see Supplemental Material).

Results

Clinical progression over one year

Patients showed weak evidence towards a significant progression of disability between baseline and year 1, as measured by EDSS ($p = 0.08$); there was a change in the MSFC subtest scores during the follow-up period, but it was not statistically significant. The clinical tests results at baseline and at one year are summarised in e-Table 1 (supplemental material).

Changes in skeletonised FA and MTR over one year

There was no significant change in skeletonised FA between baseline and one year. RD significantly increased in several regions, including the CST (cerebral peduncle bilaterally and left corona radiata), and right inferior longitudinal fasciculus, during the same follow-up, whilst AD did not change (see supplemental material for more results on these results).

Patients showed a significant reduction in skeletonised MTR over the same follow-up period in the WM along the bilateral corticospinal tracts (CST) (posterior limb of the internal capsule and cerebral peduncle), and in the genu and the body of the corpus callosum (CC) ($p < 0.01$) (**Fig. 1**). A significant decrease in MTR over time was also detected bilaterally in the thalamic radiation,

and in the superior and inferior longitudinal fasciculi ($p < 0.01$) (**Fig. 1**). Within the areas of significant change, the average difference in MTR between baseline and one year, computed across the skeleton, was 2% (mean value [SD] at baseline = 35.4 [3.1] pu, mean value [SD] at one year = 34.7 [3.3] pu).

Tract specific FA and MTR values obtained from skeletonised maps at baseline and one year are shown in **Table 1**.

Correlation between changes in FA and MTR and clinical changes over one year

Changes in FA over the follow-up period did not significantly correlate with any change in the clinical variables. AD decreases in the left CST (next to the primary motor cortex) and CC over one year correlated with changes in upper limb function, as measured by the z-NHPT scores; RD increases in WM tracts, such as the right CST (internal capsule) and CC correlated, with z-NHPT changes; RD increases in specific regions (left cingulum, left anterior thalamic radiation, body of the CC, inferior fronto-occipital fasciculus bilaterally, and left CST) also correlated with z-PASAT changes (see supplemental material for more details).

In patients, a decrease in skeletonised MTR in the genu and the body of the CC, and in the superior part of the right CST (corona radiata) was significantly correlated with reduced upper limb function, as measured by the z-NHPT scores,

over the follow-up period ($p < 0.05$) (**Fig.2**). The decrease in MTR over one year was not significantly associated with changes in EDSS, in z-TWT or in z-PASAT.

Post-hoc analysis

(i) The role of lesions

The areas of significant change in MTR were localised in part within the “new/enlarged T2 lesions” which developed over the follow-up period, but also outside them, in the NAWM (**Fig. 3**).

There was a significant correlation between the average MTR decrease over one year in the genu and the body of the CC, and in the superior part of the right CST, and the total T2 lesion load increase over the same follow-up period ($r = 0.49$, $p < 0.033$). This corresponds to an $r^2 = 0.24$, i.e. the increase in T2 lesion load can explain 24% of the variance in MTR decrease in these brain areas.

(ii) The role of total grey matter MTR

No significant correlation was found between the changes in total GM MTR over one year and the changes in clinical scores during the same period.

(iii) Correlation between FA changes and MTR decrease in regions that showed correlation between MTR changes and clinical function

No significant correlation was found between the mean FA change and the mean MTR decrease extracted from the regions of significant association between changes in MTR and changes in z-NHPT scores (i.e., the genu and the body of the CC, and from the superior part of the right CST).

Discussion

In this study, we employed a combination of MT imaging and TBSS to "skeletonise" the MTR maps and explore tract-specific microstructural changes in a unique cohort of patients with PPMS, recruited within five years of symptom onset. It is known that PPMS patients are particularly prone to show dynamic changes in their conditions in the early phase of the disease (Khaleeli et al., 2007b). Our patients showed a significant decrease in MTR along WM tracts, such as the CST, the CC, the SLF and the ILF over one year follow-up. RD (which is the average of the second and third eigenvalues of the DT) also significantly increased over time in similar regions, whilst AD (which is the principal eigenvalue of the DT) and FA did not change. We demonstrated that these very early changes were localised within the NAWM and the new or enlarged lesions visible on T2-weighted scans, which developed over the same follow-up period. Moreover, we showed that the significant decreases in MTR in the body and genu of the CC and MTR decreases in the superior part of the CST correlated with a deterioration in the upper limb function occurring over one year. Similarly, RD increases in several tracts, including the CC and the right CST (internal capsule) correlated with deterioration in the upper limb function.

The MT effect is generated by the interaction between protons localised in a relatively free environment and those whose motion is restricted (Tofts, 2003),

and MT-based imaging has been proposed as a sensitive and reliable surrogate marker of myelin content (Filippi et al., 1998; Filippi, 1999; Zivadinov, 2007). Brain areas with low MTR values (reflecting reduced efficiency in the exchange of magnetisation occurring between macromolecules and the surrounding water molecules) have been shown to correlate strongly with pathological changes in MS (Chen et al., 2007; Chen et al., 2008; Deloire-Grassin et al., 2000). In particular, post-mortem analysis of MS has demonstrated that MTR is remarkably sensitive to myelin content, in addition to axonal loss (Schmierer et al., 2004).

Given its sensitivity to the degree of tissue damage, MTR has been acquired in all subtypes of MS to investigate pathological changes in vivo (Filippi and Agosta, 2010). To date, most of the assessments have been based on the histogram-based analysis of the whole brain (Dehmeshki et al., 2001; Filippi et al., 2000) or on the investigation of *a priori* selected regions of interest (ROIs), such as the normal-appearing WM (NAWM), NA grey matter, tractography-selected WM tracts or user-defined anatomical masks (De Stefano et al., 2006; Filippi et al., 1998; Lin et al., 2008; Reich et al., 2007; Santos et al., 2002; Tur et al., 2011). In several cross-sectional studies, these approaches demonstrated significant and clinically relevant abnormalities in the NAWM of patients with PPMS (Dehmeshki et al., 2003; Filippi et al., 1999; Leary et al., 1999; Tortorella et al., 2000). A histogram-based approach has also been employed in longitudinal studies, which showed that normal-appearing brain tissues MTR at baseline predicted the deterioration of disability over time (Khaleeli et al., 2007b; Khaleeli et al., 2008).

However, there have been several attempts to develop an effective approach for performing a voxel-wise analysis of MTR images, assessing the GM compartment only or the whole brain (Audoin et al., 2007; Dwyer et al., 2009). The attractiveness of voxel-based approaches lies in the fact that they provide information about the sites of abnormality as a result of the analysis. The steps involved in image normalization and smoothing, however, might compromise the accurate localization of changes.

In order to overcome some of these limitations, in this study we propose a novel methodology that combines the sensitivity provided by MTR in detecting disease-related pathological changes with the accurate spatial information offered by TBSS. This technique allowed us to demonstrate the early accrual of tract-specific microstructural abnormalities in PPMS, specifically affecting WM tracts involved in motor function control, such as the bilateral CST, the SLF and the ILF. Indeed, the CST is the main WM pathway controlling voluntary movements, whereas the SLF and the ILF are associative tracts that have been shown to play a key role in integrating multiple functions within the complex network system that controls the precise execution of fine movements. In particular, the SLF mediates the interaction between the parietal lobe and the motor and premotor areas, which are crucial in planning movement precision in space (Koch et al., 2010), whereas the ILF, connecting the occipital cortex with the temporal cortex, is thought to be involved in the use of visual information for the purpose of guiding movements and controlling motor actions (Schmahmann and Pandya,

2007). Moreover, we have found a significant reduction in skeletonised MTR over the follow-up period in the genu and the body of the CC, where the WM fibres interconnecting motor and cognitive networks between the two hemispheres are localised. Indeed, we have recently shown in this same cohort that the early disruption of the inter-hemispheric callosal pathways may result in a disconnection syndrome that contributes to long-term physical and cognitive disability (Bodini et al., 2012). Also, in a previous cross-sectional study in this same patient cohort, we found that patients showed a diffusively reduced FA compared with controls in the NAWM (Bodini et al., 2009). Interestingly, the areas of significant FA decrease in patients at baseline, as described by our previous paper, included the bilateral CST, the CC, the thalamic radiations and the inferior longitudinal fasciculus, which are the same regions showing a further accrual of damage during the first year of follow-up. In the future it would be of interest to investigate whether there is a difference in the location and in the extent of the skeletonised MTR short-term changes between PPMS and relapse-onset MS, whose WM changes may be more related to the presence of lesions than PPMS.

Contrary to the MTR results, no significant FA changes were found over the 12 month follow-up. This suggests that MTR and FA offer complementary information when studying the evolution of brain diseases, since FA is sensitive to the detection of differences between patients and controls (Bodini et al., 2009), whereas changes in MTR correlate with changes in clinical function over one

year, suggesting that in this cohort MTR is a more sensitive marker of disease progression in early PPMS than FA. Interestingly, when we looked for changes in RD and AD over the same follow-up period, we found that there was a significant increase in RD over one year in regions which overlapped with those found using MTR, although the MTR changes were more widespread, whilst no significant changes in AD were found. This suggests that the analysis of the directional diffusivities may reflect underlying pathological changes more accurately than FA, which is obtained by combining the three eigenvalues. Although it is tempting to suggest that the observed RD and MTR changes over one year reflect increased demyelination, at least inside WM lesions (Moll et al., 2011), and especially in view of the animals studies using directional diffusivities (Song et al., 2005) and post-mortem analysis (Schmierer et al., 2004), it is likely that other processes, including axonal loss, are reflected by RD and MTR changes (Cader et al., 2007; Zhang et al., 2009; van Waesberghe et al., 1999).

With respect to correlations between imaging and clinical changes, we found that decreases in skeletonised MTR, RD and AD in the CST and in the CC significantly correlated with the deterioration in upper limb function, as measured by the z-NHPT (Cutter et al., 1999). These results extend to the PPMS population the findings of correlations between altered diffusion metrics within the pyramidal tract and motor dysfunction previously demonstrated in clinically isolated syndrome (CIS) and relapsing-remitting MS (Kern et al., 2011; Lin et al., 2007; Pagani et al., 2005; Wilson et al., 2003). Moreover, our findings support

the key role played by the disruption of callosal fibres in mediating the functional impairment of fine motor control (Bonzano et al., 2008; Johansen-Berg et al., 2007; Kern et al., 2011; Larson et al., 2002), probably through a mechanism of reduced inhibitory input (Kern et al., 2011). In addition, RD increases in the inferior longitudinal fasciculus, uncinate fasciculus, thalamic radiations and cerebellar peduncle, correlated with a deterioration of the upper limb function. These data suggest that motor dysfunction may result from the damage to a complex network of systems in MS, including the visual-motor coordination system, in which is implicated the inferior longitudinal fasciculus (Catani et al., 2003), and the control system of fine-tuning of movements during motor execution, mediated by the cerebellar structures (Voogd, 2003). In future, studies employing our TBSS-MTR methodology in combination with scores aimed at assessing individual neurological functions, such as the pyramidal and sensory scores, may test system-specific hypotheses in MS.

In addition, we found a significant inverse correlation between changes in the z-PASAT score and changes in RD in the left cingulum, left anterior thalamic radiation, body of the CC, inferior fronto-occipital fasciculus bilaterally, and in the left CST. The PASAT test is a complex working memory task involving several distinct brain areas that interact simultaneously, and is known to be heavily influenced by the disruption of connecting WM fibres in MS (Bodini et al., 2009; Audoin et al. 2005).

On the other hand, we did not find any significant correlation between changes in total GM MTR and clinical changes over one year. This finding is in line with the results of previous studies on this same cohort of patients, which reported that while total GM MTR was shown to be a useful predictor of clinical progression over a long-term follow-up period (Tur et al., 2011), WM MTR seemed to correlate better than GM MTR with short-term clinical changes (Khaleeli et al., 2007b).

Looking more closely at our results, we found that significant changes in skeletonised MTR not only included areas of newly developed or enlarged WM lesions but also regions of NAWM. In particular, we found that T2 lesion load increase over one year explained 24% of the variance in MTR decrease, suggesting that new/enlarging T2 lesions are relevant for the observed MTR drop, although they are not the only factor. Our results confirm data emerged in several studies conducted on all subtypes of MS that demonstrated the occurrence and the clinical relevance of the WM damage localised outside visible T2 lesions when using other quantitative MRI techniques (Filippi and Agosta, 2010). In addition, our data showed the development of new T2-weighted lesions and the enlargement of pre-existing ones within the areas of significant and clinically eloquent changes in skeletonised MTR, suggesting that T2 lesion load increase may contribute to the MTR decrease. This finding further underlines the already reported contribution of T2-weighted lesions to the

occurrence of the clinically relevant WM abnormalities that are picked up by changes in MTR (Vrenken et al., 2007),

A limitation of this study is that only 21 out of 50 patients included in the original cohort of 50 patients with early PPMS performed both DWI and MTR data at both baseline and one year and the lack of age- and gender-matched controls who performed the same protocol at the same time points. This limitation derives from analysis of data which were not originally acquired for the development of this specific methodology. Moreover, the differing slice thickness used for DTI and MT images should be considered as a limitation of this study, as it could potentially affect the co-registration between these images, thus compromising the accurate anatomical localisation based on TBSS. However, in order to minimise these issues, the intra-subject co-registration was optimised by the use of a cost function known to work well for images of different contrasts, namely normalised mutual information. Finally, our results need to be confirmed by future studies employing more recent, and potentially more sensitive, diffusion data acquisition protocols.

In conclusion, our 'skeletonised MTR' approach proved valuable in demonstrating the short-term accrual of microstructural damage in specific WM tracts that may contribute to clinical impairment in early PPMS. This novel method could be applied in future to explore regional microstructural WM changes in cross-sectional and longitudinal studies in patients with other forms of

MS, and with other neurological diseases. Moreover, the combination of 'skeletonised MTR' and voxel-wise measures of grey matter damage could be employed to explore the spatial and temporal relationship between the WM and the GM damage in MS as well as in other brain diseases.

Acknowledgments

The Authors are very grateful to all the patients for taking part in the study. B. Bodini was funded by the MAGNIMS/ECTRIMS fellowship. This work was undertaken at UCLH/UCL who received a proportion of funding from the Department of Health's NIHR Biomedical Research Centres funding scheme.

Tables

Table 1. Tract-specific FA and MTR values obtained from skeletonised images in patients at baseline and one-year follow-up.

Tract	baseline		Year 1	
	mean FA (SD)	mean MTR [pu] (SD)	mean FA (SD)	mean MTR [pu] (SD)
Left ATR	0.407 (0.028)	34.14 (2.81)	0.402 (0.033)	33.58 (3.28)
Right ATR	0.420 (0.032)	34.47 (2.68)	0.416 (0.042)	33.87 (3.62)
Left CST	0.521 (0.029)	35.94 (1.48)	0.570 (0.032)	35.59 (1.76)
Right CST	0.582 (0.027)	35.87 (1.44)	0.577 (0.031)	35.44 (1.59)
Left Cingulum	0.517 (0.051)	37.32 (1.45)	0.508 (0.057)	36.87 (1.60)
L Cingulum (HP)	0.456 (0.038)	33.10 (2.36)	0.456 (0.046)	31.53 (3.28)
R Cingulum (HP)	0.450 (0.043)	33.96 (1.60)	0.445 (0.054)	33.42 (1.79)
Forceps Major	0.598 (0.057)	34.84 (2.05)	0.590 (0.071)	34.58 (2.20)
Forceps Minor	0.480 (0.038)	37.46 (1.50)	0.473 (0.044)	36.96 (1.68)
Left IFOF	0.455 (0.042)	35.93 (2.09)	0.450 (0.050)	35.59 (2.17)
Right IFOF	0.455 (0.041)	35.61 (2.29)	0.449 (0.047)	35.35 (2.50)
Left ILF	0.430 (0.040)	35.65 (2.21)	0.427 (0.045)	35.49 (2.44)
Left ILF	0.447 (0.037)	35.80 (1.97)	0.440 (0.044)	35.78 (2.13)
Left SLF	0.434 (0.041)	36.84 (2.00)	0.429 (0.048)	36.51 (2.35)
Right SLF	0.445 (0.032)	36.70 (2.10)	0.441 (0.038)	36.58 (2.08)
Left UNC	0.431 (0.039)	35.67 (1.86)	0.428 (0.047)	35.44 (1.95)
Right UNC	0.448 (0.051)	35.25 (1.74)	0.446 (0.066)	35.28 (2.30)
L SLF (temporal)	0.471 (0.059)	37.11 (1.56)	0.468 (0.068)	36.83 (1.84)
R SLF (temporal)	0.505 (0.043)	36.91 (1.90)	0.496 (0.053)	36.76 (2.04)

List of Symbols: ATR = anterior thalamic radiation; CST = cortico-spinal tract; HP = hippocampal part; IFOF = inferior fronto-occipital fasciculus; ILF = inferior longitudinal fasciculus; SLF = superior longitudinal fasciculus; UNC = uncinata fasciculus; R=right; L=left.

Figure legends

Figure 1. Red voxels show the regions of significant reduction in skeletonised MTR over one year, overlaid onto the FSL fractional anisotropy template in MNI coordinates.

Figure 2. Blue voxels indicate the areas of significant correlation between the decrease in skeletonised MTR over the follow-up period and the changes in upper limb function scores (z-NHPT). The map is overlaid onto the FSL fractional anisotropy template in MNI coordinates.

Figure 3. Significant MTR changes over one year (blue) and probabilistic distribution of new/enlarged lesions over the same follow-up period in the patient group (red-yellow). The red-yellow colour scale indicates the percentage of patients who developed a new/enlarged lesion in a given voxel. This figure shows that MTR changes were not confined to areas of new/enlarged lesions, but were also detectable in the NAWM, possibly through mechanisms of Wallerian degeneration. The maps are overlaid onto the FSL T1 template in MNI coordinates.

Figure 1.

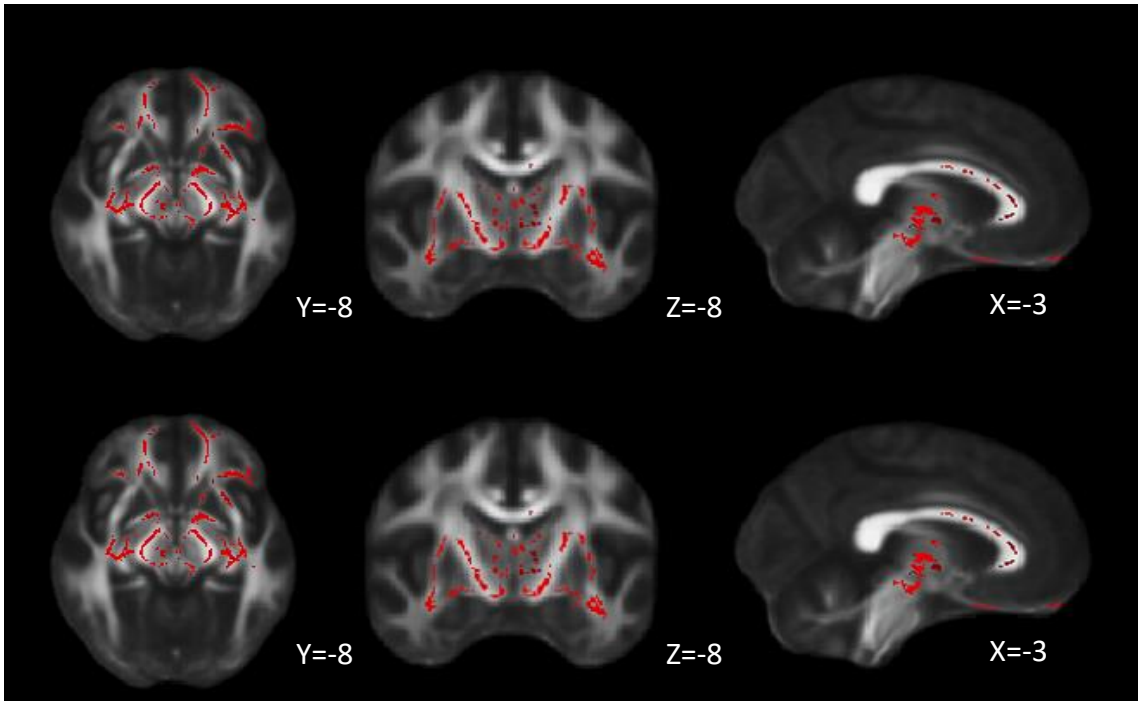


Figure 2.

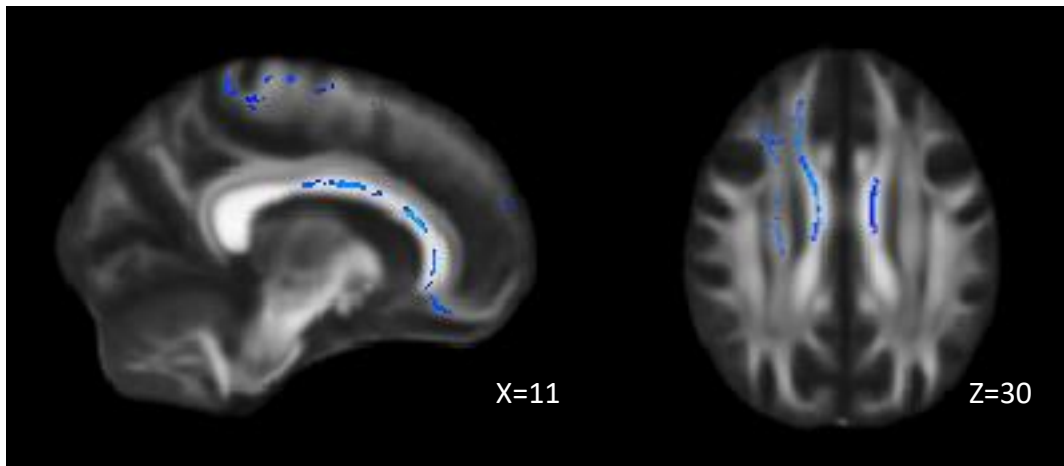
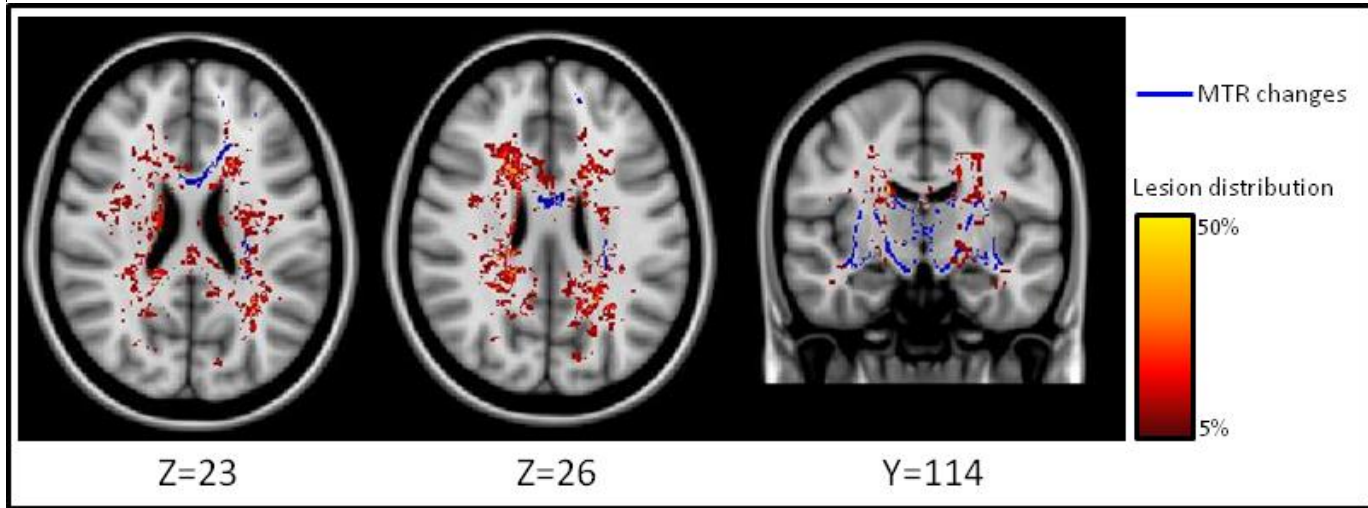


Figure 3.



References

Ashburner J, Friston KJ. 2005 Jul. Unified segmentation. *Neuroimage* 26(3):839-851.

Audoin B, Davies G, Rashid W, Fisniku L, Thompson AJ, Miller DH. 2007 May. Voxel-based analysis of grey matter magnetization transfer ratio maps in early relapsing remitting multiple sclerosis. *Mult Scler* 13(4):483-489.

Barker GJ, Tofts PS, Gass A. 1996. An interleaved sequence for accurate and reproducible clinical measurement of magnetization transfer ratio. *Magn Reson Imaging* 14(4):403-411.

Bodini B, Cercignani M, Khaleeli Z, Miller DH, Ron M, Penny S, Thompson AJ, Ciccarelli O. 2012. Corpus callosum damage predicts disability progression and cognitive dysfunction in primary-progressive MS after five years. *Hum Brain Mapp*, in press.

Bodini B, Khaleeli Z, Cercignani M, Miller DH, Thompson AJ, Ciccarelli O. 2009 Sep. Exploring the relationship between white matter and gray matter damage in early primary progressive multiple sclerosis: an in vivo study with TBSS and VBM. *Hum Brain Mapp* 30(9):2852-2861.

Bonzano L, Tacchino A, Roccatagliata L, Abbruzzese G, Mancardi GL, Bove M. 2008 Mar. Callosal contributions to simultaneous bimanual finger movements. *J Neurosci* 28(12):3227-3233.

Catani M, Jones DK, Donato R, Ffytche DH. 2003 Sep. Occipito-temporal connections in the human brain. *Brain* 126(Pt 9):2093-2107.

Chen JT, Collins DL, Atkins HL, Freedman MS, Arnold DL. 2008 Feb. Magnetization transfer ratio evolution with demyelination and remyelination in multiple sclerosis lesions. *Ann Neurol* 63(2):254-262.

Chen JT, Kuhlmann T, Jansen GH, Collins DL, Atkins HL, Freedman MS, O'Connor PW, Arnold DL. 2007 Jul. Voxel-based analysis of the evolution of magnetization transfer ratio to quantify remyelination and demyelination with histopathological validation in a multiple sclerosis lesion. *Neuroimage* 36(4):1152-1158.

Cutter GR, Baier ML, Rudick RA, Cookfair DL, Fischer JS, Petkau J, Syndulko K, Weinshenker BG, Antel JP, Confavreux C, Ellison GW, Lublin F, Miller AE, Rao SM, Reingold S, Thompson A, Willoughby E. 1999 May. Development of a multiple sclerosis functional composite as a clinical trial outcome measure. *Brain* 122 (Pt 5):871-882.

Dalby RB, Frandsen J, Chakravarty MM, Ahdidan J, Sorensen L, Rosenberg R, Videbech P, Ostergaard L. 2010 Oct. Depression severity is correlated to the integrity of white matter fiber tracts in late-onset major depression. *Psychiatry Res* 184(1):38-48.

Damoiseaux JS, Smith SM, Witter MP, Sanz-Arigita EJ, Barkhof F, Scheltens P, Stam CJ, Zarei M, Rombouts SA. 2009 Apr. White matter tract integrity in aging and Alzheimer's disease. *Hum Brain Mapp* 30(4):1051-1059.

De Stefano N, Battaglini M, Stromillo ML, Zipoli V, Bartolozzi ML, Guidi L, Siracusa G, Portaccio E, Giorgio A, Sorbi S, Federico A, Amato MP. 2006 Aug. Brain damage as detected by magnetization transfer imaging is less pronounced in benign than in early relapsing multiple sclerosis. *Brain* 129(Pt 8):2008-2016.

de Zeeuw P, Mandl RC, Hulshoff Pol HE, van EH, Durston S. 2011 Aug. Decreased frontostriatal microstructural organization in attention deficit/hyperactivity disorder. *Hum Brain Mapp*.

Dehmeshki J, Chard DT, Leary SM, Watt HC, Silver NC, Tofts PS, Thompson AJ, Miller DH. 2003 Jan. The normal appearing grey matter in primary progressive multiple sclerosis: a magnetisation transfer imaging study. *J Neurol* 250(1):67-74.

Dehmeshki J, Silver NC, Leary SM, Tofts PS, Thompson AJ, Miller DH. 2001 Mar. Magnetisation transfer ratio histogram analysis of primary progressive and other multiple sclerosis subgroups. *J Neurol Sci* 185(1):11-17.

Deloire-Grassin MS, Brochet B, Quesson B, Delalande C, Dousset V, Canioni P, Petry KG. 2000 Sep. In vivo evaluation of remyelination in rat brain by magnetization transfer imaging. *J Neurol Sci* 178(1):10-16.

Dwyer M, Bergsland N, Hussein S, Durfee J, Wack D, Zivadinov R. 2009 Jul. A sensitive, noise-resistant method for identifying focal demyelination and remyelination in patients with multiple sclerosis via voxel-wise changes in magnetization transfer ratio. *J Neurol Sci* 282(1-2):86-95.

Filippi M. 1999. Magnetization transfer imaging to monitor the evolution of individual multiple sclerosis lesions. *Neurology* 53(5 Suppl 3):S18-S22.

Filippi M, Agosta F. 2010 Apr. Imaging biomarkers in multiple sclerosis. *J Magn Reson Imaging* 31(4):770-788.

Filippi M, Iannucci G, Tortorella C, Minicucci L, Horsfield MA, Colombo B, Sormani MP, Comi G. 1999 Feb. Comparison of MS clinical phenotypes using conventional and magnetization transfer MRI. *Neurology* 52(3):588-594.

Filippi M, Inglese M, Rovaris M, Sormani MP, Horsfield P, Iannucci PG, Colombo B, Comi G. 2000 Oct. Magnetization transfer imaging to monitor the evolution of MS: a 1-year follow-up study. *Neurology* 55(7):940-946.

Filippi M, Rocca MA, Martino G, Horsfield MA, Comi G. 1998 Jun. Magnetization transfer changes in the normal appearing white matter precede the appearance of enhancing lesions in patients with multiple sclerosis. *Ann Neurol* 43(6):809-814.

Focke NK, Yogarajah M, Bonelli SB, Bartlett PA, Symms MR, Duncan JS. 2008 Apr. Voxel-based diffusion tensor imaging in patients with mesial temporal lobe epilepsy and hippocampal sclerosis. *Neuroimage* 40(2):728-737.

Giorgio A, Santelli L, Tomassini V, Bosnell R, Smith S, De SN, Johansen-Berg H. 2010 Jul. Age-related changes in grey and white matter structure throughout adulthood. *Neuroimage* 51(3):943-951.

Giorgio A, Watkins KE, Douaud G, James AC, James S, De SN, Matthews PM, Smith SM, Johansen-Berg H. 2008 Jan. Changes in white matter microstructure during adolescence. *Neuroimage* 39(1):52-61.

Johansen-Berg H, Della-Maggiore V, Behrens TE, Smith SM, Paus T. 2007. Integrity of white matter in the corpus callosum correlates with bimanual coordination skills. *Neuroimage* 36 Suppl 2:T16-T21.

Jones DK, Horsfield MA, Simmons A. 1999 Sep. Optimal strategies for measuring diffusion in anisotropic systems by magnetic resonance imaging. *Magn Reson Med* 42(3):515-525.

Kern KC, Sarcona J, Montag M, Giesser BS, Sicotte NL. 2011 Apr. Corpus callosal diffusivity predicts motor impairment in relapsing-remitting multiple sclerosis: a TBSS and tractography study. *Neuroimage* 55(3):1169-1177.

Khaleeli Z, Altmann DR, Cercignani M, Ciccarelli O, Miller DH, Thompson AJ. 2008 Nov. Magnetization transfer ratio in gray matter: a potential surrogate marker for progression in early primary progressive multiple sclerosis. *Arch Neurol* 65(11):1454-1459.

Khaleeli Z, Cercignani M, Audoin B, Ciccarelli O, Miller DH, Thompson AJ. 2007 Aug. Localized grey matter damage in early primary progressive multiple sclerosis contributes to disability. *Neuroimage* 37(1):253-261.

Khaleeli Z, Sastre-Garriga J, Ciccarelli O, Miller DH, Thompson AJ. 2007 Oct. Magnetisation transfer ratio in the normal appearing white matter predicts progression of disability over 1 year in early primary progressive multiple sclerosis. *J Neurol Neurosurg Psychiatry* 78(10):1076-1082.

Koch G, Cercignani M, Pecchioli C, Versace V, Oliveri M, Caltagirone C, Rothwell J, Bozzali M. 2010 May. In vivo definition of parieto-motor connections involved in planning of grasping movements. *Neuroimage* 51(1):300-312.

Kurtzke JF. 1983 Nov. Rating neurologic impairment in multiple sclerosis: an expanded disability status scale (EDSS). *Neurology* 33(11):1444-1452.

Larson EB, Burnison DS, Brown WS. 2002 Apr. Callosal function in multiple sclerosis: bimanual motor coordination. *Cortex* 38(2):201-214.

Leary SM, Silver NC, Stevenson VL, Barker GJ, Miller DH, Thompson AJ. 1999 Oct. Magnetisation transfer of normal appearing white matter in primary progressive multiple sclerosis. *Mult Scler* 5(5):313-316.

Lin F, Yu C, Jiang T, Li K, Chan P. 2007 Feb. Diffusion tensor tractography-based group mapping of the pyramidal tract in relapsing-remitting multiple sclerosis patients. *AJNR Am J Neuroradiol* 28(2):278-282.

Lin X, Tench CR, Morgan PS, Constantinescu CS. 2008 Apr. Use of combined conventional and quantitative MRI to quantify pathology related to cognitive impairment in multiple sclerosis. *J Neurol Neurosurg Psychiatry* 79(4):437-441.

Moll NM, Rietsch AM, Thomas S, Ransohoff AJ, Lee JC, Fox R, Chang A, Ransohoff RM, Fisher E. 2011 Nov. Multiple sclerosis normal-appearing white matter: pathology-imaging correlations. *Ann Neurol* 70(5):764-773.

Mori S, Wakana S, Nagae-Poetscher LM, van Zijl PC. 2005. *MRI Atlas of Human Brain Matter*. Amsterdam, The Netherlands.

Nguyen D, Vargas MI, Khaw N, Seeck M, Delavelle J, Lovblad KO, Haller S. 2011 Mar. Diffusion tensor imaging analysis with tract-based spatial statistics of the white matter abnormalities after epilepsy surgery. *Epilepsy Res*.

Pagani E, Filippi M, Rocca MA, Horsfield MA. 2005 May. A method for obtaining tract-specific diffusion tensor MRI measurements in the presence of disease: application to patients with clinically isolated syndromes suggestive of multiple sclerosis. *Neuroimage* 26(1):258-265.

Plummer D. 1992. DisplImage: A display and analysis tool for medical images. *Rev Neuroradiol* 5:489-495.

Raz E, Cercignani M, Sbardella E, Totaro P, Pozzilli C, Bozzali M, Pantano P. 2010 Nov. Gray- and white-matter changes 1 year after first clinical episode of multiple sclerosis: MR imaging. *Radiology* 257(2):448-454.

Reich DS, Smith SA, Jones CK, Zackowski KM, van Zijl PC, Calabresi PA, Mori S. 2006 Nov. Quantitative characterization of the corticospinal tract at 3T. *AJNR Am J Neuroradiol* 27(10):2168-2178.

Reich DS, Smith SA, Zackowski KM, Gordon-Lipkin EM, Jones CK, Farrell JA, Mori S, van Zijl PC, Calabresi PA. 2007 Nov. Multiparametric magnetic resonance imaging analysis of the corticospinal tract in multiple sclerosis. *Neuroimage* 38(2):271-279.

Ropele S, Fazekas F. 2009 Feb. Magnetization transfer MR imaging in multiple sclerosis. *Neuroimaging Clin N Am* 19(1):27-36.

Santos AC, Narayanan S, De SN, Tartaglia MC, Francis SJ, Arnaoutelis R, Caramanos Z, Antel JP, Pike GB, Arnold DL. 2002 Jun. Magnetization transfer can predict clinical evolution in patients with multiple sclerosis. *J Neurol* 249(6):662-668.

Schmahmann JD, Pandya DN. 2007 Oct. The complex history of the fronto-occipital fasciculus. *J Hist Neurosci* 16(4):362-377.

Schmierer K, Scaravilli F, Altmann DR, Barker GJ, Miller DH. 2004 Sep. Magnetization transfer ratio and myelin in postmortem multiple sclerosis brain. *Ann Neurol* 56(3):407-415.

Serra L, Cercignani M, Lenzi D, Perri R, Fadda L, Caltagirone C, Macaluso E, Bozzali M. 2010. Grey and white matter changes at different stages of Alzheimer's disease. *J Alzheimers Dis* 19(1):147-159.

Smith SM, Jenkinson M, Johansen-Berg H, Rueckert D, Nichols TE, Mackay CE, Watkins KE, Ciccarelli O, Cader MZ, Matthews PM, Behrens TE. 2006 Jul. Tract-based spatial statistics: voxelwise analysis of multi-subject diffusion data. *Neuroimage* 31(4):1487-1505.

Smith SM, Jenkinson M, Woolrich MW, Beckmann CF, Behrens TE, Johansen-Berg H, Bannister PR, De LM, Drobnjak I, Flitney DE, Niazy RK, Saunders J, Vickers J, Zhang Y, De SN, Brady JM, Matthews PM. 2004. Advances in functional and structural MR image analysis and implementation as FSL. *Neuroimage* 23 Suppl 1:S208-S219.

Smith SM, Nichols TE. 2009 Jan. Threshold-free cluster enhancement: addressing problems of smoothing, threshold dependence and localisation in cluster inference. *Neuroimage* 44(1):83-98.

Song SK, Yoshino J, Le TQ, Lin SJ, Sun SW, Cross AH, Armstrong RC. 2005 May. Demyelination increases radial diffusivity in corpus callosum of mouse brain. *Neuroimage* 26(1):132-140.

Stricker NH, Schweinsburg BC, Delano-Wood L, Wierenga CE, Bangen KJ, Haaland KY, Frank LR, Salmon DP, Bondi MW. 2009 Mar. Decreased white matter integrity in late-myelinating fiber pathways in Alzheimer's disease supports retrogenesis. *Neuroimage* 45(1):10-16.

Thompson AJ, Montalban X, Barkhof F, Brochet B, Filippi M, Miller DH, Polman CH, Stevenson VL, McDonald WI. 2000 Jun. Diagnostic criteria for primary progressive multiple sclerosis: a position paper. *Ann Neurol* 47(6):831-835.

Tofts PS. 2003. *Quantitative MRI of the brain: measuring changes caused by disease*. John Wiley and Sons.

Tortorella C, Viti B, Bozzali M, Sormani MP, Rizzo G, Gilardi MF, Comi G, Filippi M. 2000 Jan. A magnetization transfer histogram study of normal-appearing brain tissue in MS. *Neurology* 54(1):186-193.

Tur C, Khaleeli Z, Ciccarelli O, Altmann DR, Cercignani M, Miller DH, Thompson AJ. 2011 Apr. Complementary roles of grey matter MTR and T2 lesions in predicting progression in early PPMS. *J Neurol Neurosurg Psychiatry* 82(4):423-428.

Voogd J. 2003 Dec. The human cerebellum. *J Chem Neuroanat* 26(4):243-252.

Vrenken H, Pouwels PJ, Ropele S, Knol DL, Geurts JJ, Polman CH, Barkhof F, Castelijns JA. 2007 Jul. Magnetization transfer ratio measurement in multiple sclerosis normal-appearing brain tissue: limited differences with controls but relationships with clinical and MR measures of disease. *Mult Scler* 13(6):708-716.

Wilson M, Tench CR, Morgan PS, Blumhardt LD. 2003 Feb. Pyramidal tract mapping by diffusion tensor magnetic resonance imaging in multiple sclerosis: improving correlations with disability. *J Neurol Neurosurg Psychiatry* 74(2):203-207.

Wingerchuk DM, Noseworthy JH, Weinshenker BG. 1997 Nov. Clinical outcome measures and rating scales in multiple sclerosis trials. *Mayo Clin Proc* 72(11):1070-1079.

Zivadinov R. 2007 May. Can imaging techniques measure neuroprotection and remyelination in multiple sclerosis? *Neurology* 68(22 Suppl 3):S72-S82.